Cardiac Myocyte Excitation by Ultrashort High-Field Pulses

Sufen Wang,[†] Jiexiao Chen,[†] Meng-Tse Chen,[‡] P. Thomas Vernier,[‡] Martin A. Gundersen,[‡] and Miguel Valderrábano[†*]

[†]Division of Cardiac Electrophysiology, Department of Cardiology, The Methodist Hospital, Houston, Texas; and [‡]Department of Electrical Engineering-Electrophysics, University of Southern California, Los Angeles, California

ABSTRACT In unexcitable, noncardiac cells, ultrashort (nanosecond) high-voltage (megavolt-per-meter) pulsed electrical fields (nsPEF) can mobilize intracellular Ca^{2+} and create transient nanopores in the plasmalemma. We studied Ca^{2+} responses to nsPEF in cardiac cells. Fluorescent Ca^{2+} or voltage signals were recorded from isolated adult rat ventricular myocytes deposited in an electrode microchamber and stimulated with conventional pulses (CPs; 0.5–2.4 kV/cm, 1 ms) or nsPEF (10–80 kV/cm, 4 ns). nsPEF induced Ca^{2+} transients in 68/104 cells. Repeating nsPEF increased the likelihood of Ca^{2+} transient induction (61.8% for $<$10 nsPEF vs. 80.6% for $\geq$10 nsPEF). Repetitive Ca^{2+} waves arising at the anodal side and Ca^{2+} destabilization occurred after repeated nsPEF (12/29) or during steady-state single nsPEF delivery at 2 Hz. Removing extracellular Ca^{2+} abolished responses to nsPEF. Verapamil did not affect nsPEF-induced Ca^{2+} transients, but decreased responses to CP. Tetrodotoxin and KB-R7943 increased the repetition threshold in response to nsPEF: 1–20 nsPEF caused local anodal Ca^{2+} waves without Ca^{2+} transients, and $\geq$20 nsPEF caused normal transients. Ryanodine-thapsigargin and caffeine protected against nsPEF-induced Ca^{2+} waves and showed less recovery of diastolic Ca^{2+} levels than CP. Voltage recordings demonstrated action potentials triggered by nsPEF, even in the presence of tetrodotoxin. nsPEF can mobilize intracellular Ca^{2+} in cardiac myocytes by inducing action potentials. Anodal Ca^{2+} waves and resistance to Na^{+} and Ca^{2+} channel blockade suggest nonselective ion channel transport via sarcolemmal nanopores as a triggering mechanism.

INTRODUCTION

Cardiac excitation via an external electrical field requires a minimal pulse amplitude and duration. The rheobase (the minimal electric current of infinite duration able to elicit an action potential) and the chronaxie (the minimal exciting pulse duration at twice the rheobase amplitude) are classical parameters that define this concept. The conventional wisdom is that neither a pulse of infinite duration whose amplitude is below the rheobase nor a pulse of infinite amplitude whose duration is shorter than the chronaxie will elicit an action potential, given the asymptotic relationship. Thus, the amplitude threshold approaches infinity as the pulse duration approaches zero (1).

Recently, ultrashort (nanosecond), high-voltage (approximately a megavolt/m) pulsed electrical fields (nsPEF) have been shown to trigger a host of intracellular events, including intracellular Ca^{2+} mobilization in human lymphocytes (2) and Jurkat and HL-60 cells (3,4), caspase activation and apoptosis of human cells (4–6), and plasma membrane phosphatidylserine translocation in Jurkat cells (7). Recent data, as well as molecular-dynamics simulations, support the idea that transient pores in the plasma membrane (8) of nanometer scale and nanosecond duration (nanopores) underlie the mechanism of phosphatidylserine flipping. Experimental data also support ultrashort plasma membrane polarization up to ~1 V (9), large enough to create electroporation. Because pore size is thought to depend on pulse duration, nsPEF are thought to create small, resealable pores that may allow ions but not large molecules to pass through (9–11).

The effects of nsPEF on electrically excitable cells, such as neurons and cardiac myocytes, have not been fully delineated, but they potentially differ from effects on nonexcitable cells because 1), myocytes maintain large electrochemical gradients across the plasma membrane that depend on an intact lipid bilayer; 2), myocytes are endowed with voltage-sensitive channels that respond to changes in plasma membrane voltage on a submillisecond timescale; and 3), myocytes have a highly regulated intracellular Ca^{2+} cycling system that is physiologically linked to the membrane potential but also capable of independent Ca^{2+} release. We hypothesized that nsPEF leads to cardiac excitation by perturbing either intracellular Ca^{2+} cycling or electrochemical gradients at the sarcolemma. If so, nsPEF could potentially be used as an alternative mode of cardiac pacing and defibrillation. Here we show that Ca^{2+} mobilization occurs in response to nsPEF, similarly to Ca^{2+} transients that occur in response to action potentials. However, repetitive intracellular Ca^{2+} waves are also commonly induced by nsPEF. Pharmacological studies support sarcolemmal initiation via an action potential and not through direct effects on intracellular Ca^{2+} stores, which is confirmed by the demonstration of nsPEF-induced action potentials. We propose that ion movement through nonselective sarcolemmal pores plays a role in initiating nsPEF-induced action potentials.

Submitted July 10, 2008, and accepted for publication November 5, 2008.

*Correspondence: mvalderrabano@tmhs.org

Editor: David A. Eisner.

© 2009 by the Biophysical Society

0006-3495/09/02/1640/9 $2.00

doi: 10.1016/j.bpj.2008.11.011

MATERIALS AND METHODS

Cell preparation

Experiments were performed on single ventricular myocytes isolated enzymatically from adult Sprague-Dawley rats. Briefly, animals were anesthetized with 50 mg/kg pentobarbital sodium intraperitoneally and the hearts rapidly removed and retrogradely perfused at 37°C with oxygenated Tyrode's solution containing (mM): NaCl 136, KCl 5.4, $CaCl_2$ 1.8, $MgCl_2$ 1.0, NaH_2PO_4 0.33, Hepes 10, glucose 10, pH adjusted to 7.2 with NaOH. The hearts were subsequently perfused with a Ca^{2+}-free Tyrode's solution for 3 min after spontaneous contractions ceased, followed by 20–25 min perfusion with 223 U/mL collagenase (Worthington Biochemical Corp., Freehold, NJ) and 0.1 mg/mL hyaluronidase (Sigma Chemical, St. Louis, MO) in Ca^{2+}-free Tyrode's. After perfusion, the ventricles were removed into a petri dish containing ~10 mL enzyme solution with 0.02 mg/mL trypsin (Sigma Chemical), minced and triturated before being filtered through a nylon mesh (300 μm), and subsequently separated from collagenase-trypsin solution by centrifugation at 60 *g* for 30 s. Myocytes were resuspended in a sterilized Ca^{2+}-free Tyrode's to remove residual enzyme, and Ca^{2+} was slowly added back up to 1.8 mM.

To measure intracellular Ca^{2+}, cells were stained with rhod-2 AM by incubation with 10 μM dye solution at 37°C for 45 min in the presence of 0.006% pluronic acid. To measure membrane potential, cells were stained with RH237 by incubation with 12.5 μM dye solution at 37°C for 15 min. After staining, the cells were spun and resuspended in Tyrode's solution. All dyes were obtained from Invitrogen (Carlsbad, CA).

Pulse generator and delivery systems

A fast metal oxide semiconductor field effect transistor (MOSFET)-based micropulser designed and assembled at the University of Southern California was mounted on the microscope stage (Axiovert 200, Zeiss, Thornwood, NY) for delivery of 4 ns duration 10–80 kV/cm pulses directly to the microchamber electrodes in ambient atmosphere at room temperature. The microchamber is a rectangular channel of 100 μm wide, 30 μm deep, and 12 mm long, with gold-plated electrode walls, microfabricated with photolithographic methods on a glass microscope slide (Fig. 1 *A*). To directly compare "conventional pulse" (CP) stimulation (5–24 V, 0.5–2.4 kV/cm, 1 ms) with nsPEF, both pulse configurations had to be delivered via the same electrodes. We connected the nsPEF generator and a conventional stimulator (S88X, Grass, West Warwick, RI) to the same output electrodes. We designed a device with a passive diplexer circuit that acted as an "isolator" so that CPs could pass through it unaltered but nsPEF could not pass through, thereby preventing damage to the conventional stimulator (Fig. 1 *B*).

Stimulation protocols

We used two stimulation protocols: 1), S1S2 pacing, where three CP stimuli (0.5–2.4 kV/m, 1 ms, S1) at 500 ms cycle length were followed by single or multiple nsPEF (S2) at 200 ms, 400 ms, 600 ms coupling intervals; and 2), steady-state 2Hz pacing, with either CP or nsPEF delivered at 2 Hz. For nsPEF, amplitudes of 20, 40, 60, and 80 kV/cm were tested. Multiple nsPEF repetitions (two, five, 10, or 20) were delivered at 10 kHz rate (Fig. 2). The voltage and current curves created during nsPEF delivery were monitored in situ using a digital phosphor oscilloscope (Tektronix TDS3000B, with 5 gigasamples per second).

Single-cell fluorescence mapping of intracellular Ca^{2+} and membrane potential

An aliquot of Tyrode's solution (1.8 μL) with suspended cells was deposited in the microchamber, covered with a coverslip, and mounted onto the stage of an inverted microscope. Green light (520 ± 20 nm) from an X-Cite Series 120 system (Exfo, Mississauga, Ontario, Canada) was delivered via the microscope lens to the microchamber. For intracellular Ca^{2+}, fluorescence

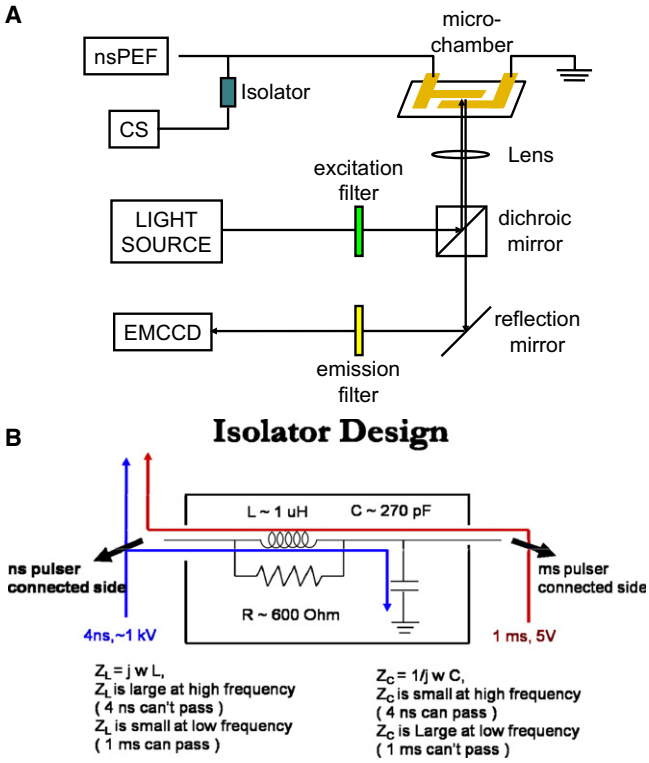

FIGURE 1 Diagram of the experimental setup. (*A*) Experimental setup. (*B*) Isolator design (a passive diplexer circuit). The 4 ns generator sees a large impedance due to the parallel inductance and resistance. The long pulse sees a low series impedance presented by the inductor. The capacitor attenuates the short pulse and leaves the long pulse unaltered. At high frequency the impedance of the inductor is large but the impedance of the capacitor is small. This blocks nanosecond pulses. At low frequencies the impedance of the inductor is small and the impedance of the capacitor is large. This allows a millisecond, kilohertz pulse to pass. The value of the inductor is ~1 μH, the capacitor has a value of 270 pF, and the resistor has a value of 600 Ohm.

was collected through a 585 ± 20 nm filter. For membrane voltage, fluorescence was collected through a 710 nm long pass filter. Both signals were recorded with an electron-multiplying CCD camera (iXon, Andor, Belfast, Northern Ireland) operating at 200 or 500 frames per second with a spatial resolution of 128 × 128 pixels. Recording was synchronized with the initiation of the stimulation, and recordings of 5 and 25 s duration were acquired for the S1S2 and 2 Hz steady-state pacing protocols, respectively. A normal Ca^{2+} transient was defined as a simultaneous rapid rise of Ca^{2+} occurring in the entire cell. Ca^{2+} waves were defined as localized rises in Ca^{2+} that propagated to the rest of the cell.

To elucidate the role of the sarcolemma and sarcoplasmic reticulum (SR) in nsPEF-induced Ca^{2+} mobilization, the following pharmacological interventions were applied: verapamil (10 μM), tetrodotoxin (TTX, 10 μM), KB-R7943 (10 μM), ryanodine (10 μM), thapsigargin (0.2 μM), and caffeine (10 mM). Verapamil, TTX, thapsigargin, and caffeine were obtained from Sigma, and KB-R7943 and ryanodine were obtained from EMD Biosciences (San Diego, CA).

Data analysis

Data were analyzed with custom software. Ca^{2+} transient amplitude was measured as the relative increase in fluorescence from onset to peak (arbitrary units). The rise time was measured from the baseline to the peak.

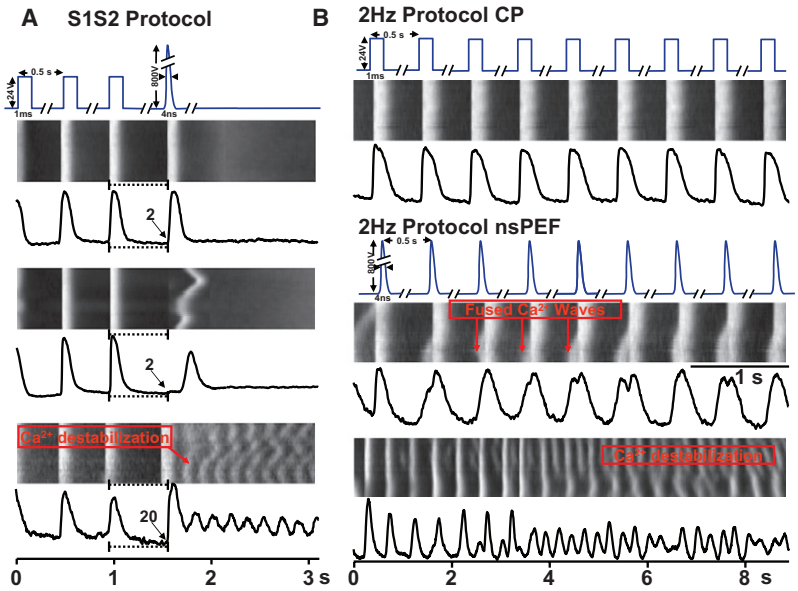

FIGURE 2 Ca^{2+} responses to different stimulation protocols. Shown are Ca^{2+} fluorescence tracings and line scans along the long axis of the cell. (*A*) S1S2 protocol: nsPEF most commonly induced Ca^{2+} transients indistinguishable from those triggered by CP (*top*). Ca^{2+} waves (anodally initiated) were also seen (*middle panel*). When repeated (20) nsPEF were delivered, consecutive Ca^{2+} waves and Ca^{2+} destabilization were generated (*bottom panel*). Numbers refer to the number of nsPEF repetitions at 10 kHz. (*B*) 2 Hz pacing protocol. In CP (*top*) each stimulus is followed by a normal Ca^{2+} transient and full recovery of diastolic Ca^{2+} levels. During 2 Hz nsPEF delivery (*middle* and *bottom panels*), Ca^{2+} transients are present (*vertical lines*) that are fused with Ca^{2+} waves and lead to Ca^{2+} destabilization. See text for details.

The time decay of the Ca^{2+} transient was calculated by single exponential fitting using Origin (Microcal, Northampton, MA) software. The recovery of diastolic Ca^{2+} levels was calculated as the ratio of trough diastolic fluorescence (after the Ca^{2+} transient) divided by the peak systolic Ca^{2+} fluorescence. All data were expressed as mean ± SD. Differences were compared using the χ^2 test, and Student's *t*-test where appropriate. Results were considered statistically significant if $p < 0.05$.

RESULTS

nsPEF-induced Ca^{2+} release

The S1S2 protocol allowed a direct comparison of Ca^{2+} responses with CP versus nsPEF in the same cell during a single recording (Fig. 2 *A*). nsPEF were delivered to myocytes at 200 ms, 400 ms, or 600 ms coupling interval after three CP beats. Seventy percent of the cells (73/104) responded to nsPEF with Ca^{2+} release. The most common response was a normal Ca^{2+} transient (Fig. 2 *A*, *top*), with comparable amplitude and nonsignificant differences in rising time and decay time from those generated by CP (amplitude ratio (S2/S1) = 1.0 ± 0.1, $n = 6$; rising time, 51.2 ± 16.1 ms vs. 48.2 ± 8.6 ms, $n = 6$; decay time constant, 111.8 ± 38.1 ms vs. 82.7 ± 20.1 ms, $n = 6$; see Fig. 6, panel *B*, group *C*). The degree of recovery of diastolic calcium levels was decreased after nsPEF (31.2 ± 6.7% of the peak amplitude) compared to CP (23.2 ± 8.0%, $p < 0.05$, $n = 6$). Cell orientation had no observable effect on the results. There was no significant impact of the S1S2 coupling intervals on Ca^{2+} release (69.2% for 200 ms, 70.6% for 400 ms, and 70% for 600 ms; Fig. 3). Multiple pulses at 10 and 20 nsPEF (delivered at 0.1 ms intervals, or 10 kHz) increased the chance of Ca^{2+} release from 63.2% (for 1, 2, 5 nsPEF, $n = 68$) to 83.3% ($n = 36$, $p < 0.01$). Besides normal Ca^{2+} transients, nsPEF-induced Ca^{2+} responses included Ca^{2+} waves that could be isolated (Fig. 2 *A*, *mid panel*; see Movie S1 in the Supporting Material) or repetitive, consistent with Ca^{2+} destabilization (Fig. 2 *A*, *bottom*; Movie S2). The most common patterns of Ca^{2+} release of 1, 2, 5 nsPEF on Ca^{2+} cycling were normal transients (42/43). Repetitive Ca^{2+} waves and Ca^{2+}

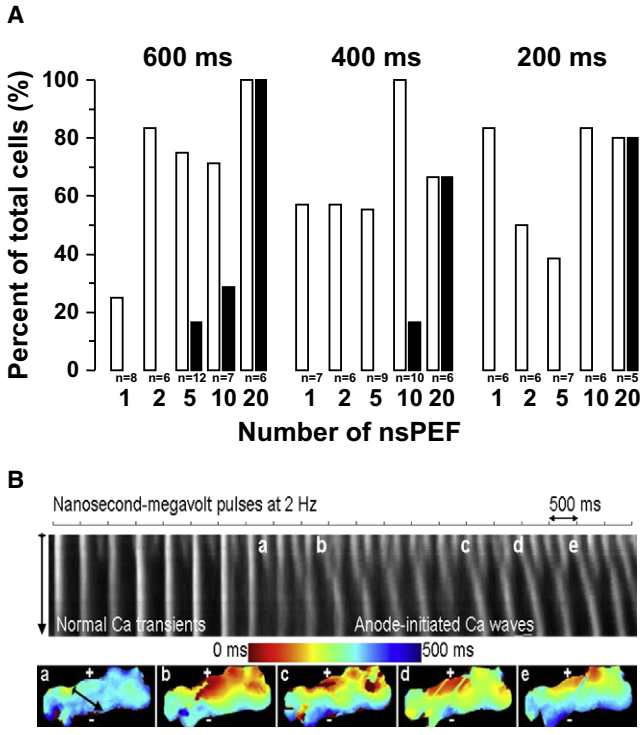

FIGURE 3 (*A*) Responses of cells to nsPEF at different S1S2 coupling intervals. Open bars represent Ca^{2+} transients, and closed bars represent Ca^{2+} waves. (*B*) Representative cell isochronal intracellular Ca^{2+} propagation maps of anodally initiated Ca^{2+} waves.

destabilization were more frequently observed in 10 and 20 nsPEF (1/68 of 1, 2, 5 nsPEF vs. 13/36 of 10, 20 nsPEF, $p < 0.001$). Fig. 3 *A* shows the rate and type of Ca^{2+} responses obtained with different S1S2 coupling intervals and different nsPEF pulse repetitions. Myocytes would not survive after the initiation of repetitive spontaneous Ca^{2+} waves or Ca^{2+} destabilization. Although it is hard to calculate a threshold for cell destruction, it was dose-dependent: with increasing nsPEF repetition, the probability of damage increased (Fig. 3 *A*). Fourteen of the 73 responding cells were damaged by the presence of Ca^{2+} waves (all receiving ≥ 5 nsPEF), and the remaining 59 showed no visible damage. Thus the survival rate of nsPEF stimulation was 80.8%.

Conventional 2 Hz pacing led to Ca^{2+} transients with each paced beat (Fig. 2 *B*, *top*). Upon termination of pacing, a quiescent state was regained. The threshold for CP capture was measured as 13.7 ± 5.8 V in 22 cells. Single nsPEF at 2 Hz were then delivered in the same cell for comparison. The nsPEF amplitudes tested were 20, 40, 60, 80 kV/cm. There was a dose response: Ca^{2+} release was rarely found with 20 kV/cm pulses (1/6), and rose to 54.5% (6/11) with 40 kV/cm and to 100% with 60 and 80 kV/cm nsPEF (21/21, $p < 0.001$). Therefore, the amplitude threshold for single nsPEF-induced Ca^{2+} transient formation was 60 kV/cm in the steady-state pacing protocol. Upon initiation of 2 Hz, single nsPEF pacing, there was a variable latency period of 2.12 ± 3.33 s (range: 0–5.45 s), followed by Ca^{2+} release consistent with normal transients after each nsPEF. However, after several transients, Ca^{2+} waves started to arise (3.95 ± 2.67 s after nsPEF initiation) consistently at the anodal side of the cell; they appeared to precede nsPEF-induced Ca^{2+} transients and fused with them (Fig. 2 *B*, *mid panel*, Fig. 3 *B*, and Movie S3). The timing of the anodal Ca^{2+} wave was not consistently synchronized to the nsPEF, nor were the Ca^{2+} transients after Ca^{2+} waves arose. Fig. 3 *B* and Movie S2 show isochronal intracellular Ca^{2+} propagation maps of anodal-initiated Ca^{2+} waves. However, individual, anodal-initiated Ca^{2+} waves were limited, and ultimately, upon continuation of 2 Hz nsPEF pacing, Ca^{2+} destabilization occurred (21.59 ± 9.03 s after nsPEF stimulation, $n = 7$), characterized by multiple Ca^{2+} waves of chaotic and ever-changing propagation patterns (Fig. 2 *B*, *bottom*, and Movie S3). Thus, prolonged suprathreshold nsPEF delivery at 2 Hz uniformly leads to cell destruction.

We then performed a systematic study of pharmacological interventions to explore potential mechanisms of nsPEF-induced Ca^{2+} release. We tested drugs using both the S1S2 and steady-state protocols, using nsPEF parameters that were shown to uniformly lead to effects: for the S1S2 protocol we used a coupling interval of 400 ms and 10 repetitions of 80 kV/cm nsPEF delivered at 10 kHz, and for the steady-state protocol we used single 80 kV/cm delivered at 2 Hz. CP stimulation at 24V 1 ms was used as control.

Contribution of transsarcolemmal Ca^{2+} entry to nsPEF-induced Ca^{2+} release

To identify the mechanism for nsPEF effects on intracellular Ca^{2+}, the extracellular medium was investigated as a possible source for Ca^{2+} released after nsPEF. Myocytes suspended in normal Tyrode's solution ([Ca^{2+}] 1.8 mM) were centrifuged, resuspended in Tyrode's with zero Ca^{2+}, and rapidly (1–2 min) transported onto the microscope stage. Ca^{2+} release was inhibited completely for both CP and nsPEF. A typical behavior is shown in Fig. 4. Therefore, both CP-induced Ca^{2+} release and nsPEF-induced Ca^{2+} release require external Ca^{2+}.

Considering the fact that nsPEF induced normal Ca^{2+} transients, similar to those triggered by CP (that is, by an action potential), it is logical to assume that Ca^{2+} entered normally via the L-type Ca^{2+} channel upon nsPEF stimulation. We performed experiments using the two protocols outlined above in the presence of the voltage-dependent Ca^{2+} channel blocker verapamil (10 μM). Using the S1S2 protocol during verapamil exposure, nsPEF-induced Ca^{2+} transients had significantly greater amplitude than those induced by CP (amplitude ratio (S2/S1) = 2.8 ± 2.2, $n = 10$, $p < 0.05$), with unremarkable changes in rising time and delay time (rising time, 59.2 ± 16.3 ms ($n = 12$) vs. 50.1 ± 9.5 ms ($n = 10$), $p = 0.12$; decay time constant, 72.4 ± 16.3 ms ($n = 12$) vs. 83.0 ± 17.5 ms ($n = 10$), $p = 0.14$), consistent with verapamil-induced depression of the CP-induced Ca^{2+} transient (as expected), but with failure to affect nsPEF-induced Ca^{2+} release (see Figs. 4 and 6).

We further tested whether Ca^{2+} release results from an action potential by decreasing cell excitability. We tested the Ca^{2+} response in the presence of TTX (10 μM). As expected, TTX abolished the response to CP. Initial testing included 10 nsPEF in the S1S2 protocol (400 ms coupling

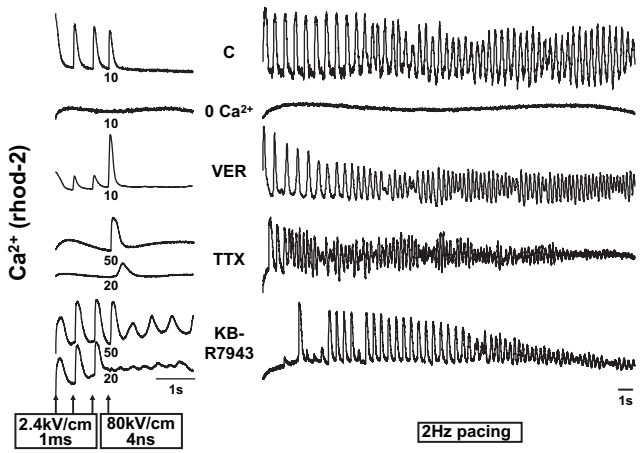

FIGURE 4 Typical responses of intracellular Ca^{2+} in response to CP and nsPEF in the presence of different pharmacological interventions that interfere with transsarcolemmal Ca^{2+} entry. C: control; TTX: tetrodotoxin; VER: verapamil. See text for details.

interval). With these settings, 10 nsPEF induced a Ca^{2+} transient only in 1/6 cells. In 5/6 cells, increasing nsPEF pulse repetition was performed: 20 nsPEF induced a local anodal Ca^{2+} wave that propagated variably into the cell in 5/6 cells without inducing a whole-cell transient. Increasing nsPEF pulse number to 50 pulses generated a Ca^{2+} transient, with persistent anodal Ca^{2+} waves (Fig. 5 *A*). Thus, nsPEF were able to overcome effects of TTX, but requiring higher than control pulse repetition (10/10 cells in control had Ca^{2+} transients using 10 pulses at 400 ms S1S2 coupling interval versus 1/6 with TTX, $p = 0.001$). Increasing pulse repetition to 20 pulses led to anodal Ca^{2+} waves, and increasing repetition to 50 led to Ca^{2+} transients.

We then hypothesized that the generation of nsPEF-induced Ca^{2+} transients involves several steps: 1), the creation of nanopores (8–10,12)—most pronounced at the anodal side—that persist beyond nsPEF and allow nonselective ion exchange; 2), ion channel transport driven passively by the preserved electrochemical gradient (mostly Na^+ and Ca^{2+}), which then depolarizes the membrane; 3), secondary activation of voltage-sensitive Na^+ channels to threshold and generation of an action potential; and 4), a contribution of electrogenic reverse Na^+/Ca^{2+} transport contributing to secondary Na^+ entry and depolarization. Consistent with this interpretation, blockade by TTX of Na^+ channel activation unmasks local Ca^{2+} entry, more pronounced at the anodal side, and leads to local Ca^{2+} waves via Ca^{2+}-induced Ca^{2+} release.

We then evaluated the role of reverse Na^+/ Ca^{2+} exchange in triggering nsPEF-induced action potentials using KB-R7943 (10 μM). KB-R7943 is an isothiourea derivative that has been reported to selectively and potently block the Ca^{2+} influx through the reverse mode of the cardiac Na^+/Ca^{2+} exchanger rather than the forward mode (13). As opposed to TTX, KB-R7943 did not affect responses to CP. However, like TTX, it increased the nsPEF repetition threshold required for nsPEF to elicit a response (8/9 cells required 20 or more nsPEF). With increased pulse repetition, local anodal Ca^{2+} waves were also induced (Fig. 5 *B*). Similar results were obtained by substituting Li^+ for Na^+ in the extracellular medium (data not shown).

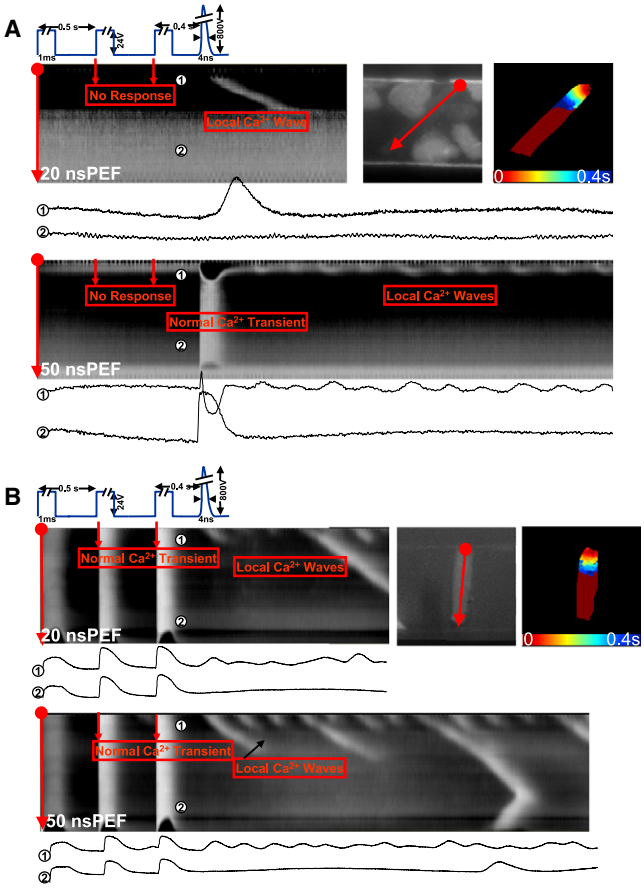

FIGURE 5 Localized Ca^{2+} waves in response to nsPEF. (*A*) In the presence of TTX, there is no response to conventional stimulation. Repeated nsPEF lead to an anodal Ca^{2+} wave (20 nsPEF repetitions) or to a Ca^{2+} transient followed by anodal Ca^{2+} waves (50 nsPEF repetitions). (*B*) In the presence of KB-R7943, the response to conventional stimulation is unaffected (normal Ca^{2+} transients), but nsPEF repetition leads to a localized Ca^{2+} wave (10 nsPEF and 50 nsPEF repetitions).

Effects of SR disabling on nsPEF-induced Ca^{2+} release

The combination of ryanodine and thapsigargin is known to disable the SR by inhibiting Ca^{2+} uptake and release. We compared Ca^{2+} transient characteristics of CP and nsPEF in the presence of ryanodine and thapsigargin. Compared to control, slower Ca^{2+} transient decay time constants for both CP- and nsPEF-induced Ca^{2+} transients were observed (CP, 149.0 ± 50.9 ms with ryanodine-thapsigargin (n = 10) vs. 82.7 ± 20.1 ms in control (n = 6), p = 0.001; nsPEF, 334.8 ± 183.1 ms (n = 10) with ryanodine-thapsigargin vs. 111.8 ± 38.1 ms in control (n = 6), p = 0.01). In 10/10 myocytes tested, comparing Ca^{2+} transients induced by nsPEF versus CP stimulation, nsPEF-induced Ca^{2+} transients were shown to have a slower rising time, longer decay time constant, and higher amplitude (rising time, 105.9 ± 35.3 ms vs. 75.0 ± 25.1 ms, n =10, p = 0.04; decay time constant, 334.8 ± 183.1 ms vs. 149.0 ± 50.9 ms, n = 10, p = 0.008; amplitude ratio (S2/S1) = 1.2 ± 0.1, n = 10; Fig. 6). The fact that Ca^{2+} does not return to diastolic levels after nsPEF during ryanodine-thapsigargin exposure compared to CP suggests that nsPEF-induced Ca^{2+} transients pose more Ca^{2+} load to the SR than the load created by CP.

When SR Ca^{2+} was depleted with the use of caffeine, the decay time slowed down dramatically with an unchanged rising time compared to control, as expected (decay time, 318.0 ± 116.0 ms vs. 111.8 ± 38.1 ms, n = 6, p = 0.001; rising time, 59.3 ± 12.3 ms vs. 51.2 ± 16.1 ms, n = 6, p = 0.18). nsPEF-induced Ca^{2+} transients had less

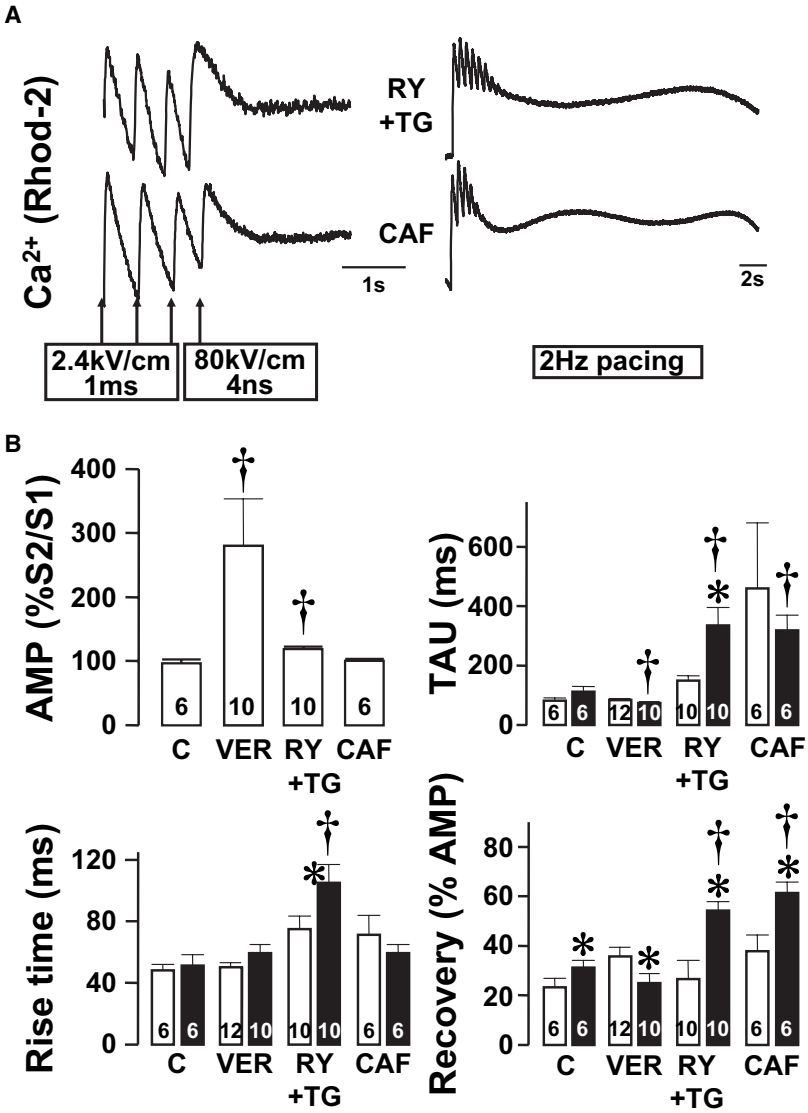

FIGURE 6 (*A*) Typical behavior of intracellular Ca^{2+} in response to different pharmacological interventions that interfere with SR function. (*B*) Comparisons of Ca^{2+} transient parameters between S1 and S2 in the presence of different interventions. (AMP: amplitude; TAU: time decay constant; RY+TG: ryanodine+thapsigargin; CAF: caffeine; VER: verapamil). Open bars represent S1, closed bars represent S2, * $p < 0.05$ vs. S1 by *t*-test; † $p < 0.05$ vs. control (*C*) by *t*-test.

recovery of diastolic Ca^{2+} levels than those created by CP (trough diastolic Ca /peak systolic Ca, 61.4 ± 9.6% vs. 37.8 ± 14.5%, $n = 6$, $p = 0.02$). This is also consistent with an increased Ca^{2+} load generated by nsPEF.

When the 2 Hz protocols were used, both ryanodine-thapsigargin and caffeine led to decreasing responses to nsPEF: after a few Ca^{2+} transients, the cells became refractory (Fig. 6 *A*, *right panel*). As opposed to control, no Ca^{2+} waves were observed upon repeated 2 Hz nsPEF stimulation, suggesting that Ca^{2+} waves and Ca^{2+} destabilization require functional Ca^{2+} cycling and are probably secondary to sarcolemmal Ca^{2+} entry induced by nsPEF.

Sarcolemmal membrane voltage changes during nsPEF exposure

It is challenging to record optical maps of membrane potential in single myocytes. Simultaneous recording of intracellular Ca^{2+} and membrane potential by using dual staining with rhod-2 AM and RH237 was not feasible due to decreased fluorescence signal changes during dual staining. We were able to record isolated RH237 fluorescence in five cells under control conditions and three cells with TTX using the S1S2 protocol (Fig. 7). The results indicate that nsPEF can create an action potential similarly to CP. Furthermore, in the presence of TTX, with 50 pulse repetitions nsPEF could trigger an action potential, whereas CP could not (Fig. 7).

DISCUSSION

This study produced several major findings. nsPEF can generate Ca^{2+} transients similar to those created by CP, and this involves generation of action potentials. Thus, interventions that completely abolish action potentials (e.g., zero extracellular Ca^{2+}) eliminate the response to nsPEF. However, multiple findings suggest that nsPEF lead to

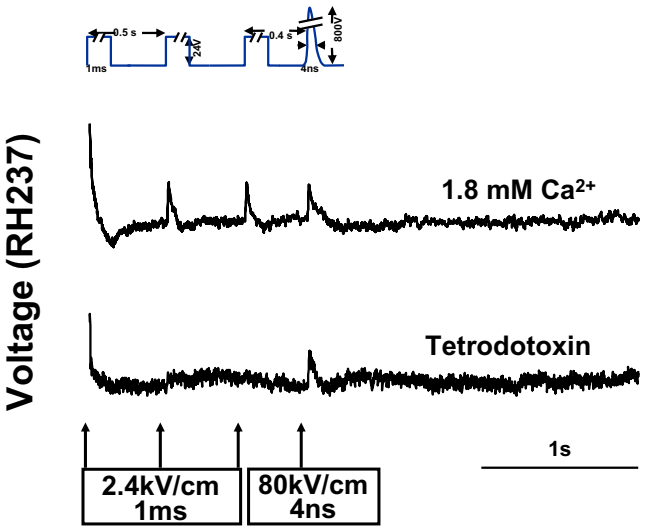

FIGURE 7 Typical membrane potentials of myocytes treated with (*A*) 1.8 mM Ca^{2+} and (*B*) TTX (10 μM).

cardiac excitation via a mechanism different from membrane polarization-induced activation of ion channels (as with CP), and point to poration as the main mechanism.

Cardiac myocyte response to field stimulation

Cardiac cell excitation in response to pulsed field stimulation has been studied in a limited range of pulse durations and strengths. When pulse parameters similar to the CP used in our study are employed, cell excitation occurs asymmetrically in the cell. Hyperpolarization and depolarization occur at the anodal and cathodal cell poles, respectively (14,15). Cathodal depolarization leads to activation of I_{Na} and initiation of an action potential. Anodal hyperpolarization leads to an inward I_{K1} current that secondarily acts to depolarize the cell (16). Thus, it is the response of voltage-sensitive ion channels that mediates excitation by CP.

The response is nonlinearly related to field strengths and durations. Using different ranges of pulse durations and field strengths, Sharma et al. (16) found that short pulses (0.5 and 1 ms) had a paradoxical loss of excitation at high field strengths. This was related to excessive positive polarization at the cathodal pole—to potentials more positive than the I_{Na} reversal potential—that caused the cathodal Na^+ current to be outward and hyperpolarizing. In long pulses, high field strengths were able to excite the cell due to the modulatory effects of the inward I_{K1} current, but not in short pulses. Ultrashort pulses were not studied, but these results would support less excitability (as mediated by ion channels) when very high field strengths are used with short pulse duration.

High field strengths have been associated with electroporation (17). Previous work has shown that poration in cardiac myocytes occurs with a plasma membrane voltage of ~300–400 mV (18). Furthermore, electroporation is a graded process in cardiac cell membranes that increases with increasing membrane voltage (19). Cheng et al. (14) showed that during high-field pulses of long durations (several milliseconds), the myocyte response had two components. The rapid response was hyperpolarizing at the anodal cell pole and depolarizing at the cathodal pole, as described above (14,15). The slower, time-dependent response had a time course that varied in slope with field strength, and was associated with postshock depression of the action potential plateau and local hypercontractions in the hyperpolarized end. This second phase was attributed to electroporation, as suggested by computer simulations (14). By showing propidium iodine uptake in cell strands, Cheek and Fast (20) proved that electroporation caused this response. Sharma and Tung (15) found that responses consistent with electroporation were more common at high field strengths. Therefore, it appears solidly proven that high field strengths lead to electroporation, which has also been shown to play a role in the whole-heart response to defibrillation shocks (21,22). However, none of these studies used ultrashort pulsed fields; instead, they used pulse parameters expected to excite cells via ion current activation.

By extrapolating from the data of Sharma et al. (16), one can conclude that very high field pulses of very short duration fail to excite cardiac myocytes through activation of depolarizing currents, because of excessive positive polarization at the cathodal pole to potentials more positive than the I_{Na} reversal potential. However, extremely high field strengths are expected to cause electroporation.

Cardiac myocyte excitation by nsPEF

It is unclear whether the time responsiveness of voltage-sensitive ion channels is fast enough to react to a 4 ns intense polarization. In our study, several facts argue against excitation via direct ion current activation and support secondary excitation by electroporation. First, nsPEF-induced excitation is not consistent with an all-or-none pattern; rather, there seems to a dose-dependent or cumulative effect. Increasing nsPEF repetition increases the likelihood of response. Second, a graded response to nsPEF is shown when single nsPEF are delivered at 2 Hz: from an initial latency of no response, to the induction of paced Ca^{2+} transients, to the induction of Ca^{2+} waves, followed by Ca^{2+} destabilization. None of these are present in CP at 2 Hz, and suggest cumulative poration that culminates in cell Ca^{2+} destabilization. Recent work indicates that nsPEF-induced poration leads to prolonged increased conductance of the plasma membrane (23), which could lead to this cumulative effect. Computer simulations also support the persistence of nsPEF-induced pores (24). Third, nsPEF effects are resistant to verapamil and create a higher than normal (CP-induced) Ca^{2+} entry to be claimed by the SR (less recovery of diastolic Ca^{2+} levels). We believe nsPEF-induced Ca^{2+} transients have an additional source of Ca^{2+} through poration that is not

blocked by verapamil. Fourth, although nsPEF repetition can overcome the effects of TTX, this drug leads to local anodal Ca^{2+} entry and local Ca^{2+} waves, which may represent the unmasked trigger for cardiac excitation when TTX is not present. Fifth, reverse Na^+/ Ca^{2+} exchange blockade decreases responsiveness to nsPEF and also leads to local anodal Ca^{2+} entry and local Ca^{2+} waves, suggesting that electrogenic Na^+/Ca^{2+} exchange plays a role in nsPEF-induced cardiac excitation.

The mechanism of action potential generation by nsPEF is complex, but is likely to involve electroporation leading to nonselective Na^+ and Ca^{2+} entry, with the former leading to secondary activation of Na^+ channels to threshold and the latter leading to reverse Na^+/Ca^{2+} exchange. These data challenge the traditional concept of chronaxie and demonstrate what to our knowledge is a new, indirect mechanism of cardiac excitation. Although electroporation during field stimulation has been abundantly shown in previous studies, those studies used longer stimuli—long enough to directly activate ion currents. Our findings support what we believe is a novel indirect excitation mechanism by pore-mediated ion transfer and secondary ion current activation.

Ca^{2+} response to nsPEF in excitable myocytes versus nonexcitable mammalian cells

Ca^{2+} mobilization in response to nanosecond high-voltage pulses was recently observed in nonexcitable mammalian cells (2–4); however, the mechanism is not well understood. Vernier et al. (2) showed nsPEF-induced increases in the intracellular Ca^{2+} concentration in human lymphocytes. The Ca^{2+} burst was uniform across the cell, originated within the cytoplasm, and was not the propagation of a Ca^{2+} wave from a disturbance in the plasma membrane, based on the limits of resolution of their observations at ~100 ms and 0.4 μm. Beebe et al. (3) reported that the nsPEF induced an increase in intracellular Ca^{2+} that was similar to purinergic agonist-mediated Ca^{2+} release from intracellular stores, which secondarily initiated capacitive Ca^{2+} influx through store-operated Ca^{2+} channels in the plasma membrane. Their experiments support the hypothesis that in nonexcitable cells, pulses with high voltage (>10 kV/cm) and durations below the plasma membrane charging time constant lead to Ca^{2+} release from poration of intracellular stores. However, the hypothesis that differences in charge time between the plasma membrane and intracellular organelles make the former ''transparent'' to nsPEF and the latter more sensitive to charging and poration has been discredited, since plasma membrane polarization has been proven (9). Studies in excitable chromaffin cells suggest that Ca^{2+} entry via the plasma membrane may also be the source of Ca^{2+} increases (25).

The results from cardiac myocytes in this study were complex. Most commonly, Ca^{2+} mobilization in response to nsPEF was generated at the sarcolemma via an action potential. We believe our data are consistent with an indirect mechanism of action potential generation, involving the creation of nonselective, short-lasting nanopores (persisting long enough to allow ion entry) that lead to subsequent passive cation entry into the cell. In previous studies (14,26), electroporation was reported to lead to local anodal Ca^{2+} entry and local hypercontractions. This in turn depolarizes the membrane to threshold over time (a process that requires functional Na^+ channels) and activates reverse Na^+/Ca^{2+} exchange; the end result is the generation of an action potential that has increased Ca^{2+} entry. In control conditions, an increased amplitude of the Ca^{2+} transient was not apparent with nsPEF, but a decreased recovery of diastolic Ca^{2+} levels was demonstrable. Disabling SR function and blocking L-type Ca^{2+} channel demonstrated the additional Ca^{2+} load created by nsPEF compared to CP. Impairing activation of Na^+ channels increased the repetition threshold of nsPEF-induced Ca^{2+} transients, and unmasked local Ca^{2+} entry as shown by anodally induced Ca^{2+} waves. We believe the local Ca^{2+} waves created by repeated nsPEF in the presence of TTX reflect passive Ca^{2+} entry via nanopores. Under TTX influence, Ca^{2+} and Na^+ entry via nanopores is not able to activate Na^+ channels to threshold, yet local Ca^{2+} entry can generate Ca^{2+}-induced Ca^{2+} release. The fact that local Ca^{2+} waves occurred consistently at the anodal side of the cells is likely linked to the higher voltages (and increased poration) created at this side (9). With higher pulse repetition, even with TTX, action potentials were created. This interpretation is further reinforced by the data obtained using KB-R7943, which, like TTX, increased the nsPEF pulse repetition threshold but, unlike TTX, did not affect responses to CP. In this case, KB-R7943 impaired the generation of an action potential by nsPEF, suggesting that reversed Na^+/ Ca^{2+} exchange plays a role in depolarizing the cell after Ca^{2+} enters the cell via nsPEF-induced pores.

During steady-state 2 Hz nsPEF delivery, ''paced'' Ca^{2+} transients and Ca^{2+} waves appeared desynchronized with nsPEF delivery. Desynchronization of Ca^{2+} transients suggests that the creation of action potential is not triggered by direct nsPEF-induced membrane polarization to threshold. Rather, action potentials leading to Ca^{2+} transients occur whenever Na^+ and Ca^{2+} transport through pores leads to depolarization to threshold, which may not occur instantaneously. Similarly, Ca^{2+} waves may require a critical Ca^{2+} concentration that may not be achieved instantaneously at every nsPEF delivery.

CONCLUSIONS

We have demonstrated that ultrashort, high-field, low-energy pulses can indirectly lead to cardiac cell excitation via a mechanism involving poration. These results challenge the concept of chronaxie. The use of nsPEF technology to excite cardiac cells and mobilize intracellular Ca^{2+} may prove valuable for cardiac pacing and defibrillation.

SUPPORTING MATERIAL

Three movies and their legends are available at http://www.biophysj.org/biophysj/supplemental/S0006-3495(08)00777-7.

This project was supported by a grant from the National Institutes of Health (R21HL085215, ''Nanosecond-Megavolt Pulse Technology for Cardiac Stimulation and Defibrillation''). M.V. was also supported by a grant from the Houston Texans.

All authors have read the manuscript and take responsibility for its content. There are no conflicts of interest.

REFERENCES

1. Stokes, K. B., and G. N. Kay. 2001. Artificial electrical cardiac stimulation. *In* Clinical Cardiac Pacing and Defibrillation. K. A. Ellenbogen, G. N. Kay, and B. Wilkoff, editors. Saunders, Philadelphia 17–52.
2. Vernier, P. T., Y. Sun, L. Marcu, S. Salemi, C. M. Craft, et al. 2003. Calcium bursts induced by nanosecond electric pulses. *Biochem. Biophys. Res. Commun.* 310:286–295.
3. Beebe, S. J., P. F. Blackmore, J. White, R. P. Joshi, and K. H. Schoenbach. 2004. Nanosecond pulsed electric fields modulate cell function through intracellular signal transduction mechanisms. *Physiol. Meas.* 25:1077–1093.
4. Beebe, S. J., J. White, P. F. Blackmore, Y. Deng, K. Somers, et al. 2003. Diverse effects of nanosecond pulsed electric fields on cells and tissues. *DNA Cell Biol.* 22:785–796.
5. Beebe, S. J., P. M. Fox, L. J. Rec, E. L. Willis, and K. H. Schoenbach. 2003. Nanosecond, high-intensity pulsed electric fields induce apoptosis in human cells. *FASEB J.* 17:1493–1495.
6. Vernier, P. T., L. Aimin, L. Marcu, C. M. Craft, and M. Gundersen. 2003. Ultrashort pulsed electric fields induce membrane phospholipid translocation and caspase activation: differential sensitivities of Jurkat T lymphoblasts and rat glioma C6 cells. *IEEE Trans Dielect Elect Ins.* 10:795–809.
7. Vernier, P. T., Y. Sun, L. Marcu, C. M. Craft, and M. A. Gundersen. 2004. Nanoelectropulse-induced phosphatidylserine translocation. *Biophys. J.* 86:4040–4048.
8. Vernier, P. T., M. J. Ziegler, Y. Sun, M. A. Gundersen, and D. P. Tieleman. 2006. Nanopore-facilitated, voltage-driven phosphatidylserine translocation in lipid bilayers–in cells and in silico. *Phys. Biol.* 3:233–247.
9. Frey, W., J. A. White, R. O. Price, P. F. Blackmore, R. P. Joshi, et al. 2006. Plasma membrane voltage changes during nanosecond pulsed electric field exposure. *Biophys. J.* 90:3608–3615.
10. Chen, N., K. H. Schoenbach, J. F. Kolb, R. James Swanson, A. L. Garner, et al. 2004. Leukemic cell intracellular responses to nanosecond electric fields. *Biochem. Biophys. Res. Commun.* 317:421–427.
11. Hu, Q., R. P. Joshi, and K. H. Schoenbach. 2005. Simulations of nanopore formation and phosphatidylserine externalization in lipid membranes subjected to a high-intensity, ultrashort electric pulse. *Phys. Rev.* 72:031902.
12. Hu, Q., S. Viswanadham, R. P. Joshi, K. H. Schoenbach, S. J. Beebe, et al. 2005. Simulations of transient membrane behavior in cells subjected to a high-intensity ultrashort electric pulse. *Phys. Rev.* 71:031914.
13. Iwamoto, T., T. Watano, and M. Shigekawa. 1996. A novel isothiourea derivative selectively inhibits the reverse mode of Na^+/Ca^{2+} exchange in cells expressing NCX1. *J. Biol. Chem.* 271:22391–22397.
14. Cheng, D. K., L. Tung, and E. A. Sobie. 1999. Nonuniform responses of transmembrane potential during electric field stimulation of single cardiac cells. *Am. J. Physiol.* 277:H351–H362.
15. Sharma, V., and L. Tung. 2002. Spatial heterogeneity of transmembrane potential responses of single guinea-pig cardiac cells during electric field stimulation. *J. Physiol.* 542:477–492.
16. Sharma, V., R. C. Susil, and L. Tung. 2005. Paradoxical loss of excitation with high intensity pulses during electric field stimulation of single cardiac cells. *Biophys. J.* 88:3038–3049.
17. Jones, J. L., R. E. Jones, and G. Balasky. 1987. Microlesion formation in myocardial cells by high-intensity electric field stimulation. *Am. J. Physiol.* 253:H480–H486.
18. Tovar, O., and L. Tung. 1992. Electroporation and recovery of cardiac cell membrane with rectangular voltage pulses. *Am. J. Physiol.* 263:H1128–H1136.
19. Tung, L. 1996. Detrimental effects of electrical fields on cardiac muscle. *Proc. IEEE.* 84:366–378.
20. Cheek, E. R., and V. G. Fast. 2004. Nonlinear changes of transmembrane potential during electrical shocks: role of membrane electroporation. *Circ. Res.* 94:208–214.
21. Al-Khadra, A., V. Nikolski, and I. R. Efimov. 2000. The role of electroporation in defibrillation. *Circ. Res.* 87:797–804.
22. Nikolski, V. P., A. T. Sambelashvili, V. I. Krinsky, and I. R. Efimov. 2004. Effects of electroporation on optically recorded transmembrane potential responses to high-intensity electrical shocks. *Am. J. Physiol.* 286:H412–H418.
23. Pakhomov, A. G., J. F. Kolb, J. A. White, R. P. Joshi, S. Xiao, et al. 2007. Long-lasting plasma membrane permeabilization in mammalian cells by nanosecond pulsed electric field (nsPEF). *Bioelectromagnetics.* 28:655–663.
24. Smith, K. C., and J. C. Weaver. 2008. Active mechanisms are needed to describe cell responses to submicrosecond, megavolt-per-meter pulses: cell models for ultrashort pulses. *Biophys. J.* 95:1547–1563.
25. Vernier, P. T., Y. Sun, M. T. Chen, M. A. Gundersen, and G. L. Craviso. 2008. Nanosecond electric pulse-induced calcium entry into chromaffin cells. *Bioelectrochemistry.* 73:1–4.
26. Knisley, S. B., and A. O. Grant. 1995. Asymmetrical electrically induced injury of rabbit ventricular myocytes. *J. Mol. Cell. Cardiol.* 27:1111–1122.